ISSN 2047-0371

2.4.2. Terrain analysis and landform recognition

Calogero Schillaci[1], Andreas Braun[1] & Jan Kropáček[1]

[1]Department of Geosciences, Tuebingen University, Germany (calogero.schillaci@student.uni-tuebingen.de)

ABSTRACT: In the last decades, Geographic Information Systems (GIS) allowed the detailed analysis of land surface, whereas the development in Remote Sensing (RS) offered increasingly detailed Digital Elevation Models (DEMs) and multispectral imagery. This combination fostered a rapidly evolving research in the field of geomorphology. In this contribution, a workflow for a Digital Terrain Analysis (DTA) is introduced, based on a free open source software (FOSS) called SAGA, and an overview on landform recognition and extraction from DEMs provided. Furthermore, a variety of DEM data sources are outlined, on which the multiscale DTA can be performed. An overview of DEMs, pre-processing and visualization techniques are elaborated and a case study in the Ethiopian highlands is used to compare three different resolution DEMs (90, 30, 2 m) in terms of their potential for: visual analysis, landform characterization and hydrological application. A typical workflow for the generation of primary and secondary terrain derivatives is therefore illustrated, as well as landform identification, as well as a description of the challenges and problems that can occur in this context.

KEYWORDS: Digital Terrain Analysis; Landforms; SAGA; SRTM; Digital Elevation Models

Introduction

Terrain analysis

The aim of Terrain Analysis (TA) is the explanation of the arrangement of the Earth's surface as well as their classification based on the surface pattern similarities (Strahler, 1957; Wilson and Gallant, 2000). Landforms can be defined as specific geomorphic features on the Earth, ranging from large-scale features (such as plains and mountain ranges) to minor features (such as individual gullies, faults and valleys), both man-made or from natural genesis which have a defined range of physical and visual characteristics (for a complete description see Goudie, 2004).

Before the introduction of Digital Elevation Models (DEMs), landforms were only manually identified by means of surveys when available through interpretation of aerial photographs (Garbrecht and Martz, 2000). During the 19th and early 20th century, the study of the landforms aimed at the production of physiography maps (Thornbury, 1965; Graf, 1987). Since World War I, aerial photographs were extensively used to give a view of the enemy's area, aiming at a description of the landforms (Pavlopoulos *et al.*, 2009). During this period, aircraft were equipped with cameras to record enemy movements. Technological advances in the photogrammetry and aerial photography interpretation were made in this time frame and boosted the geomorphological field of research.

In the late 20th century when the computing capacity of processors improved, DEMs have regularly been used for geomorphological investigations. Research was conducted on the effect of spatial resolution and the quality of the obtained derivatives (Chairat and Delleur, 1993; Zhang and Montgomery, 1994; Garbrecht and Martz, 2000; Pike, *et al*., 2008).

Through TA, it is possible to achieve a qualitative and quantitative description of landforms (Florinsky, 2012). Therefore achieving a morphographical characterization of the terrain (Klimaszewski, 1982) that represents the appearance and shape of the features. Within the last forty years, physical

geography research has used TA techniques for the topographic analysis and visualization of the land surface features. This includes: drainage pattern extraction; river morphology (e.g. Peucker and Douglas, 1975; O'Callaghan and Mark, 1984; Skidmore, 1989; Smith *et al.,* 1990; Band, 1993); watershed delineation (e.g. Jenson and Domingue, 1988; Band, 1986); surface roughness assessment (e.g. Grohmann *et al.,* 2010); monitoring the slope movements (e.g. Wieczorek and Snyder, 2009); predicting the spatial distribution of gully erosion, and soil texture (e.g. Zakerinejad and Maerker, 2014).

TA represents an established application that allows for the extraction of landforms and their qualitative and quantitative spatial assessment (Wilson, 2012). In particular, the availability of worldwide medium-resolution DEMs and the rapid development of different digital stereo photogrammetry software has allowed the extraction of detailed DEMs. Consequently, software (outlined in Table 1), tailored workflows and user-friendly toolboxes have been developed (Abera *et al.*, 2014), allowing geographers and geomorphologists their complete use.

Table 1: Software for Digital Terrain Analysis

Software	Information	Source
SAGA GIS	Free and open source, runs on Windows and Linux Focuses raster processing, support of various formats Highly specialized DTA	http://www.saga-gis.org
QGIS	Free and open source, user friendly Focuses both raster and vector processing Basic DTA, but growing pool of user-scripted extensions	http://www.qgis.org
MicroDEM	Freeware, runs on Windows Focuses raster processing, recommended for advanced users Many applications related to DEMs	http://www.usna.edu/Users/oceano/pguth/website/microdem/microdem.htm
ERDAS Imagine	Commercial, one of the leading products in remote sensing Very user friendly and stable processing Terrain module including basic and advanced DTA	http://www.hexagongeospatial.com/products/remote-sensing/erdas-imagine
VisualSFM	Freeware, runs on Windows, Linux and Mac OSX Allows the 3D reconstruction of point sources and images Limited documentation (still in progress)	http://ccwu.me/vsfm/
Agisoft PhotoScan	Commercial, but leading software for photogrammetric use Allows the 3d reconstruction of various input source data Large documentation and support	http://www.agisoft.com

Landform recognition

Different studies have proposed various definitions of landforms (Speight, 1990; Milne *et al.*, 1995). Those converge in the definition of landforms as a *uniform element* in terms of the geomorphometric similarity (Minár *et al.*, 2013). Geomorphic thresholds are at the base of any landform recognition (Schumm, 1979). Mathematically, hillslopes have been investigated as a continuous surface made up by neighboring objects. Those objects or units have been classified from geographer in two ways: i) based on their geometry (classical approach); and, ii) based on their semantics, i.e. classes chosen and named by the scientist´s contexts and aims (Dehn *et al.*, 2001).

With the arrival of DEMs at a middle resolution (5-30 cell size), attempts have been made towards an automated and hierarchical subdivision of the terrain into homogenous units (Dikau, 1989). The latter defined the *facets* as landform units defined by a homogenous profile and plan curvature. The concept of landform classification has been established, assigning rules (thresholds) to the DEM first and second derivatives

To improve Dikau's (1989) methodology (based on a square nearest neighbor research), Brabyn (1998) developed a methodology based on a circle nearest neighbor pixel search. He suggested the use of a circular-searching window, rather than a square to remove the problem related to the

microrelief representation. In this overview, the work of Evans (2012) on the specific geomorphometry of glacial cirques and drumlins should also be mentioned. His pioneering work was about programming computers on the automatic calculation of morphometric features, such as slope and other parameters using both manual measures and DEM-based attributes. Despite these landforms not being present in the study area, there are visual distinctive landscape units and have been studied for paleo-glaciology issues (Smith *et al.*, 2009).

Regarding Karst landforms, McIlroy de la Rosa (2012) gives an extensive overview of digital classifications at different scales, as well as suitable techniques. At the macroscale level remote sensing, photogrammetry or LiDAR are named as best options for DEM generation. Examples for the classification of fluvial landforms are given by Gilvear *et al.* (1999), Ramasamy and Paul (2005), Large and Heritage (2012), and Javernick *et al.* (2014).

Erosion landforms have gained a growing interest in the last decades due to their large off-site impacts on cultivated and residential lands (Valentin *et al.*, 2005) and the potential for low-cost monitoring (Marzolff and Poesen, 2009). The study of erosion landform development has brought researchers to define functional approaches to predict their future activity and spatial distribution (Märker *et al.*, 2011), the latter attempt to derive Erosion Response Units (Sidorchuk *et al.,* 2003) from sophisticated machine learning and statistical approaches.

Prima *et al.* (2006) have carried out an example of regional scale automated landform classification in a volcanic environment. The methodology employed was a supervised classification of morphometric derivatives (slope and topographic openness) to achieve quantitative landform classification.

The remainder of the chapter will discuss the data capture and pre-processing that need to be undertaken, the terrain attributes methods available and then present a GIS case study highlighting how these are implemented.

Data capture (DEM sources) and pre-processing

There are several software options for TA, these are summarized in Table 1. This article will focus on the System for Automated Geo-Analysis (SAGA, open source GIS).

Table 2: Sources of DEMs at various scales

Dataset	Spatial resolution	Use in geomorphology	Suitable scale	Source and price	Notes
SRTM C	1 arc-sec (90 m)	Regional overview of landforms, landscape type, regional tectonic structures (main faults)	1:100,000	USGS/EROS Data Center, CGIAR (void-filled version). Free of charge	Two versions available original and filled void.
SRTM C (2014)	3 arc-secs (30 m)	Landforms, drainage pattern	1:25,000	EROS / NASA/ JPL. Free of charge.	Released in 2014
SPOT	20 m	Landforms, drainage pattern	1:25,000	ISIS/CNES 10€/km² (Scene)	Processed on-demand.
ALOS PRISM	10 m	Landforms, drainage pattern, surface roughness, volumes calculation	1:15,000	Image triplet from ESA (Third Part Mission). ESA grant (50 euro) scene about1125 km^2	Processed in Leica Photogrammetry-suite.
Aerial Photos	2 m	Landforms, detailed drainage pattern, surface roughness, fault scarps, volume calculation, gullies, riverine morphology	1:5,000	Local mapping agency or authorities. Costs may vary.	Processed by Structure from Motion (SFM). Mostly acquired with metric cameras

Several DEMs have been used for TA research (summarized in Table 2). Valid examples that can support TA and landform recognition are represented by the global DEM, such as SRTM-C DEM 90 m spatial resolution (±20 m error at 90% confidence) and SRTM-C 30 m spatial resolution (± 16 m at 90% confidence) (Farr *et al.*, 2007). At a regional scale, ALOS PRISM DEM with resolution 10 m spatial resolution (±5 m at 90% confidence) based on satellite stereo photogrammetry (Tadono *et al.*, 2014), and, the local DEM with 2 m spatial resolution (±3 m at 90% confidence) resolution, based on aerial stereo photogrammetry Structure from Motion (SfM) (Westoby *et al.*, 2012).

Independent of the DEM's source, pre-processing is a required step to avoid artificial spikes and isolated pixels that will affect the generated surface (Wang and Liu, 2006). Automatically generated DEMs often have artifacts, which represent local alteration of the land surfaces, arising from different factors such as feature matching techniques, coarse spatial resolution or reconditioning by anthropic structures, i.e. buildings or bridges. These are often just a few pixels large, but they can cause problems with hydrological modeling. Wang and Liu (2006) have provided an accurate description of the nature/behaviour of surface depressions. Therefore, an algorithm called "*Fill Sinks*" can be applied to a DEM to prevent faulty results.

However, especially for high resolution DEMs, artificial structures such as bridges can serve as unwanted drainage barriers and represent causes of large sinks (Figure. 1.) In this case, manual editing of the DEM has to be performed according to the workflow illustrated in Figure 2

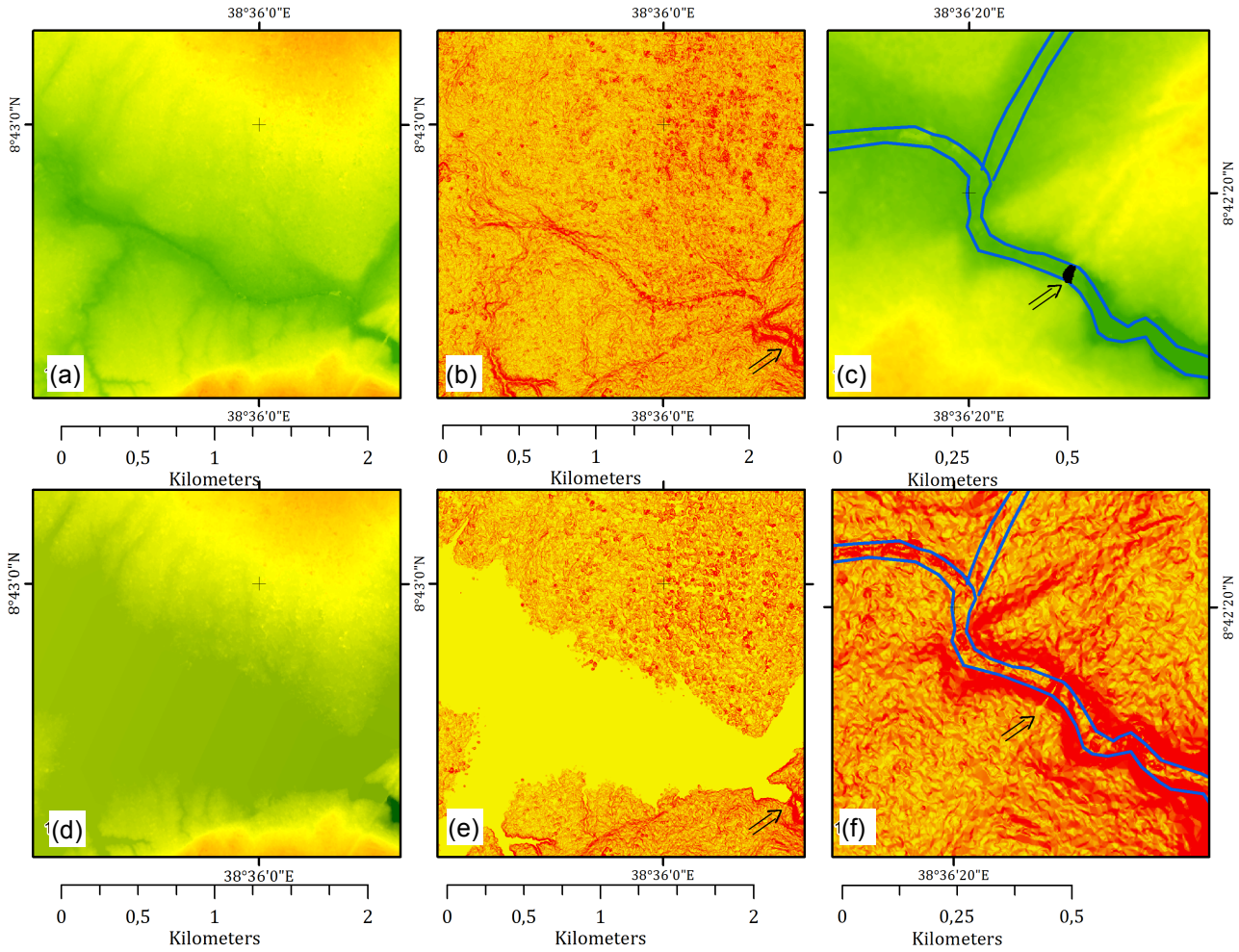

Figure 1: Pre-processing of the high resolution DEM: (a) the original SfM DEM, (b) the derived slope map, (c) shows the unwanted object, in this case represented by a bridge, that has to be removed to avoid (d) the SfM after Fill sink (Wang and Liu, 2006) and (e) the slope map derived with a huge "dam effect". Finally, (f) shows the result of the Fill sink after the tool "Burn stream network" in the DEM (SAGA).

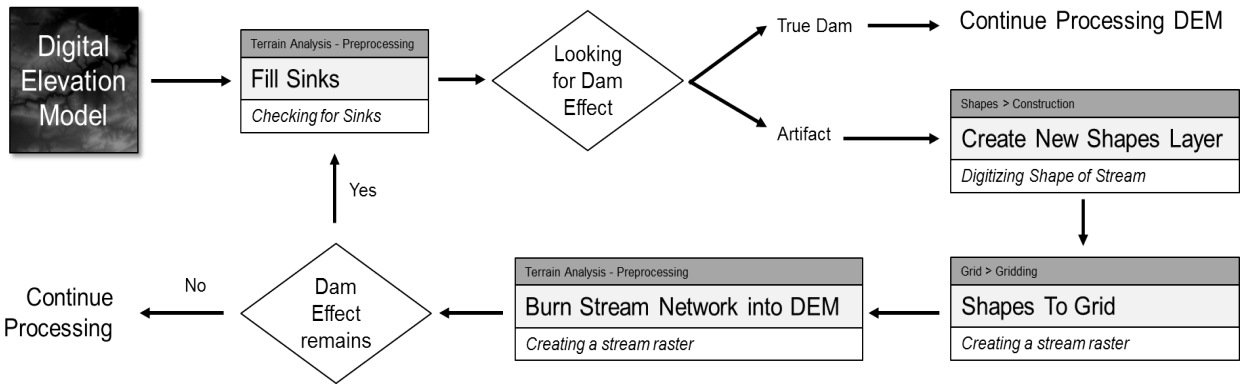

Figure 2: Workflow for the elimination of the "dam effect" in SAGA GIS.

In a first step to the removal of unwanted barriers, the erroneous barrier has to be identified in the DEM. Comparing the slope of the terrain before and after the removal of sinks (Figure 1) can show if errors were caused by artificial structures. These occur as extensive plains, mostly along valleys. In this case, the user has to digitize a new line (or polygon), which intersects the unwanted barrier. After converting the digitized vector into a grid, the SAGA module "*Burn Stream Network into DEM*" can be executed. It decreases the topography along the digitized line by a certain height. This decrease in altitude is expressed by the variable '*epsilon*' in SAGA and has to be chosen by the user. Afterwards, the algorithm "*Fill Sinks*" will not interpret the area upstream of this structure as a basin any longer.

Overview of the most used terrain analysis attributes and landforms recognition methods

This section introduces the different domains of TA that are of interest to geomorphologists. This will start with basic topographic derivatives, determinants and terrain parameters, and later will proceed to more complex indices and hydrological parameters.

Digital topography

The topographic surface can be described as a continuous function, where z is the elevation and x and y are the Cartesian coordinates:

$$z = f(x, y) \qquad \text{Eq. 1}$$

The simplest measure of topography is the **altitude** itself. It is important for the visibility of topographic features and the distribution of temperature, rainfall or vegetation.

To enhance the interpretability of the elevation raster, a **shaded relief** or hillshade, is often generated first. Shaded relief is a visually pleasing representation of the terrain (Marston and Jenny, 2015). It assumes an illumination of the raster surface given at a defined direction and angle of the light source. Before the digital era, it was performed manually by darkening shaded areas in a map. Its application for analytical reasons has several possible calculations, which are outlined by Lukas and Weibel (1995).

Contour lines represent another possibility of visualizing the spatial distribution of elevations in the DEM. They are therefore often used in maps to give the reader an impression of the terrain without using too many colours or signatures. They can be generated based on a DEM by the minimum curvature approach suggested by Fogg (1985). However, the scale at which contour lines are generated is crucial as they significantly under-represent the areas between the chosen intervals, especially in areas of low relief (Hutchinson and Gallant, 1999). As a rule of thumb, the spacing between the contour lines should be at least twice the pixel size of the DEM (*Hengl et al.*, 2003).

Hydrology

One of the main questions in hydrology addresses the interaction of surface water and topography. Speight (1974) proposed a method for the digital delineation of watersheds. His concept of catchment area

(CA) calculation strongly influenced hydrological modelling; using slope and curvature to generate potential flow directions at the Earth's surface. These directions were then used to estimate borders of separate catchments. By adding up potential water flow (flow accumulation), a drainage network can be derived (Zeverbergen and Thorne, 1987). This was already seen as a measure for landscape dissection by Horton (1945) and can be expressed as drainage density, indicating the total length of the streams related to an area (m/m²).

These findings were later used to calculate hierarchical river systems, proposed by Strahler (1957) as the **Strahler order**. They are used to define stream size, based on a scaling hierarchy of tributaries. An indicator for the potential water content and horizon depth of the soil is the **Topographic Wetness Index** (TWI) by Beven *et al.* (1979), used for the quantification of topographic control on hydrological processes (Sørensen *et al.,* 2006). This is calculated by the following equation:

$$\text{TWI} = ln\frac{CA}{tan(G)}, \qquad \text{Eq. 2}$$

where CA is the local upslope area draining through the cell and where tan(G) is the local slope in radians.

Morphometry

The two most important morphometric parameters are slope inclination and slope aspect; these are the basic flow attributes of the Earth's surface that are used to derive more complex features (Florinsky, 2012). **Slope gradient** (often referred to as *slope*) is the angle G between the tangent plane P and the horizontal plane S at a given point of the topographical surface (Lehmann, 1816). It is determined by the following equation:

$$G = \arctan\sqrt{p^2 + q^2}, \qquad \text{Eq. 3}$$

Where $\mathrm{p} = \frac{\partial z}{\partial x}$ and $\mathrm{q} = \frac{\partial z}{\partial y}$

Equation 3 is calculated in degrees, however percentage values are also common. However, it has to be kept in mind that 100% are corresponding to 45° because this is the angle in which vertical and horizontal differences are equal.

Slope aspect (referred to from now on as *aspect*) is a clockwise angle A from north to a projection of the external normal n to the horizontal plane S at a given point of the Earth's surface (Marida 1972). It determines measures of insulation, temperature, vegetation, soil characteristics and moisture.

$$G = -90(1 - sgn(q)](1 - |sgn(p)|) + 180[1 + sgn(p)] - \frac{180}{\pi} sgn(p)\arccos\left(\frac{-q}{\sqrt{p^2+q^2}}\right), \qquad \text{Eq. 4}$$

It is measured in degrees, whereby 0° is equal to North and 180° is equal to South.

Local curvature is a measure of the surface roundness of an area. It can be divided into horizontal curvature k_h (*plan curvature*) and vertical curvature k_v (*profile curvature*) (Wilson and Gallant, 2000). **Plan curvature** is a measure of flow convergence ($k_h < 0$) and divergence ($k_h > 0$) and determines soil water or the deposition of particles. **Profile curvature** controls water flow acceleration ($k_h > 0$) and deceleration ($k_h < 0$) and therefore the erosion potential of an area (Shary, 1991). They can be described by the following equations:

$$k_h = \frac{p^2 r + 2pqs + q^2 t}{(p^2+q^2)\sqrt{1+p^2+q^2}} \qquad \text{Eq. 5}$$

$$k_v = \frac{q^2 r - 2pqs + p^2 t}{(p^2+q^2)\sqrt{(1+p^2+q^2)^3}}, \qquad \text{Eq. 6}$$

where $\mathrm{t} = \frac{\partial^2 z}{\partial y^2}$ and $s = \frac{\partial^2 z}{\partial x \partial y}$.

Many other derivatives of curvatures exist (mean curvature, excess curvature, ring curvature or tangential curvature, for example) but they all rely on the same principles (Florinsky, 2012).

Morphology

DEMs can also be used to distinguish between different landforms. One way is to describe the **surface roughness** of areas. This parameter refers to the variability in elevation within a defined radius and is therefore very sensitive to the selected scale. It is used for the identification of coherent structures or underlying processes (Hobson, 1972). Many approaches have been developed to calculate surface roughness and each of them fits into a certain application. Grohmann *et al.* (2010) compare five different types of roughness: area ratio,

vector dispersion, the absolute standard deviations (SD) of elevation, slope and profile curvature. This was completed for different DEM resolutions to extract topographic information. They conclude that area ratio operates most independently of scale, therefore being more suitable when coarser resolution DEMs are applied.

Besides the relative comparison of surfaces according to their roughness, there are also algorithms, which directly address whole types of landforms. For example, the **Fuzzy landform element classification** is an unsupervised continuous classification method (McBratney and De Gruijter, 1992). It was first implemented by Zadeh (1965). Since a landform's behaviour can be defined as continuous, the fuzzy classification algorithm can satisfactorily describe them (Zadeh, 1965). This classification creates clusters that can have a partial membership to the nearest cluster. Several parameters are needed in order to perform the fuzzy classification algorithm, and, the presence of the elevation avert the misclassification of flat ridges from valleys (Irvin *et al.*, 1997). The identification of proper fuzzy rules for an unbiased mapping of terrain forms was shown by Haider *et al*. (2015) on example of mapping of peneplains.

Case study

The workflow presented in the case study will be extended to the most used terrain derivatives calculation Figure. 3, used for geomorphology investigations. The general TA workflow introduced previously showed what can be achieved in terms of interpretation of relief forms, feature extraction and hence the calculation of the basic terrain attributes for hydrological modelling in a friendly, used environment, such as SAGA.

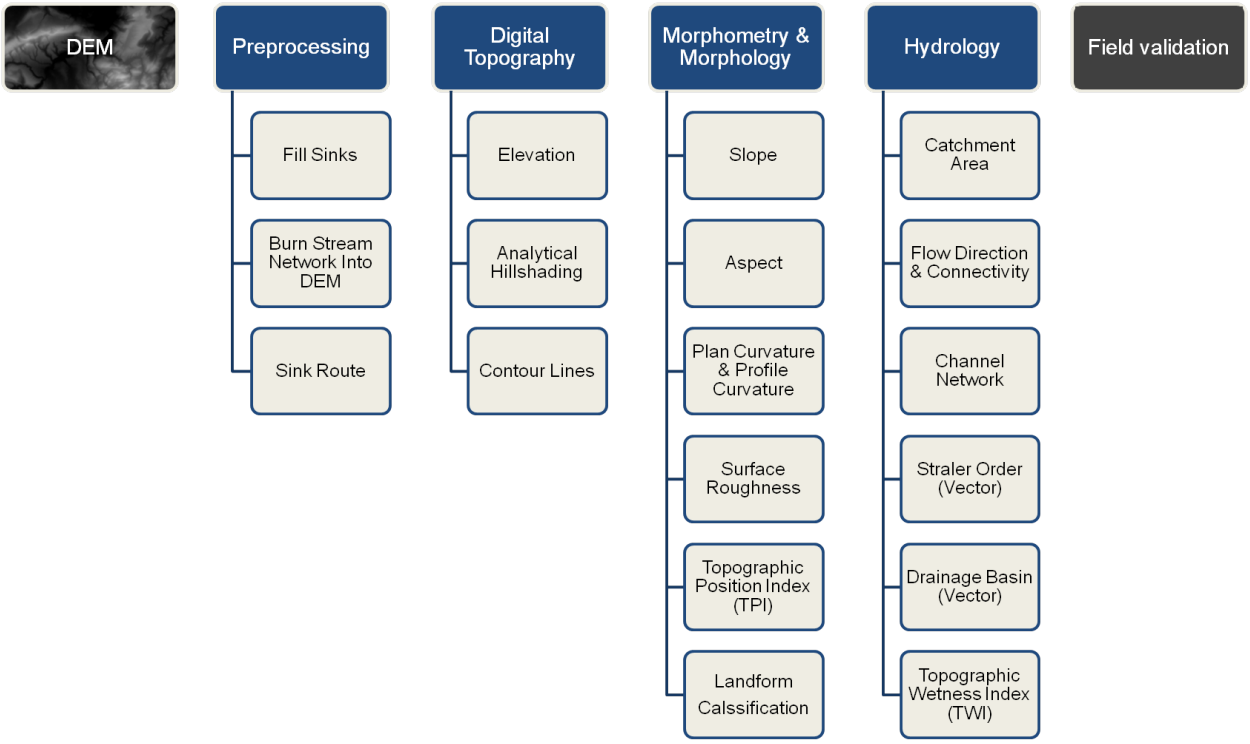

Figure 3: Workflow in SAGA GIS.

Three DEM sources were compared to assess their suitability for the automatic delineation of landforms and the terrain features at certain scales. Based on the case study a discussion of the workflow and calculation of various land surface parameters with the following DEMs:

i. SRTM - 3 arcsec, 90 m
ii. SRTM C - 1 arcsec, 30 m
iii. SfM DEM - 2 m

The three DEMs were selected based on representative scales used in geomorphological mapping (Figure 1).

Furthermore, we intended to provide a visual comparison of 10 terrain derivatives.

34 aerial images taken in 1972 were used for this case study, obtained from the Ethiopian Mapping Agency EMA, as scanned photographs (1200 dpi) and were processed with the software PhotoScan Agisoft, (Professional Edition). With this methodology, camera positions and orientation were solved automatically. The resulting DEM allowed coverage of the whole study area.

The selected study area is located in the Upper Awash River Basin, Southwest of Addis Ababa, Ethiopia (Figure 4). This site was chosen due to: i) the form and features diversity (heterogeneity); and, ii) the availability of a wide range of spatial scales DEM (from the middle to the high resolution). The study site is approximately 64 km² in area, with the altitude varying between 1850 and 2200 m above sea level.

Software

All the analyses in this article were performed in SAGA GIS; a software package licensed under the General Public Licence (GNU). The first release of SAGA was in 2004 at the Department for Physical Geography at the University of Göttingen. Two volume manuals have been provided by the SAGA working group (Cimmery, 2010a, 2010b), which give an insight to the software utilities

Figure 4: Study area of the case study

Results

Hillshade and contour lines

Terrain Analysis > Lighting > Analytical Hillshading

Shapes - Grid > Contour Lines from Grid

When performing a hillshade or slope function in any GIS, the elevation units are presumed to be the same as the horizontal units. Therefore, working in a projected coordinate system based on meter units (e.g. UTM) is compulsory (Florinsky, 2012).

Current scientific publications often feature an automatically generated hillshade map (analytical hillshade) to quickly demonstrate relief features. Hereby a new raster is created illustrating lighter and darker areas, depending on the topography, which is easily recognizable as a 3D surface for the human eye

In contour lines, 10 m line spacing has been chosen. Figure 5 shows the shaded relief of the study area with contour lines; there is an increase in spatial resolution in Figure 5 (a, b and c).

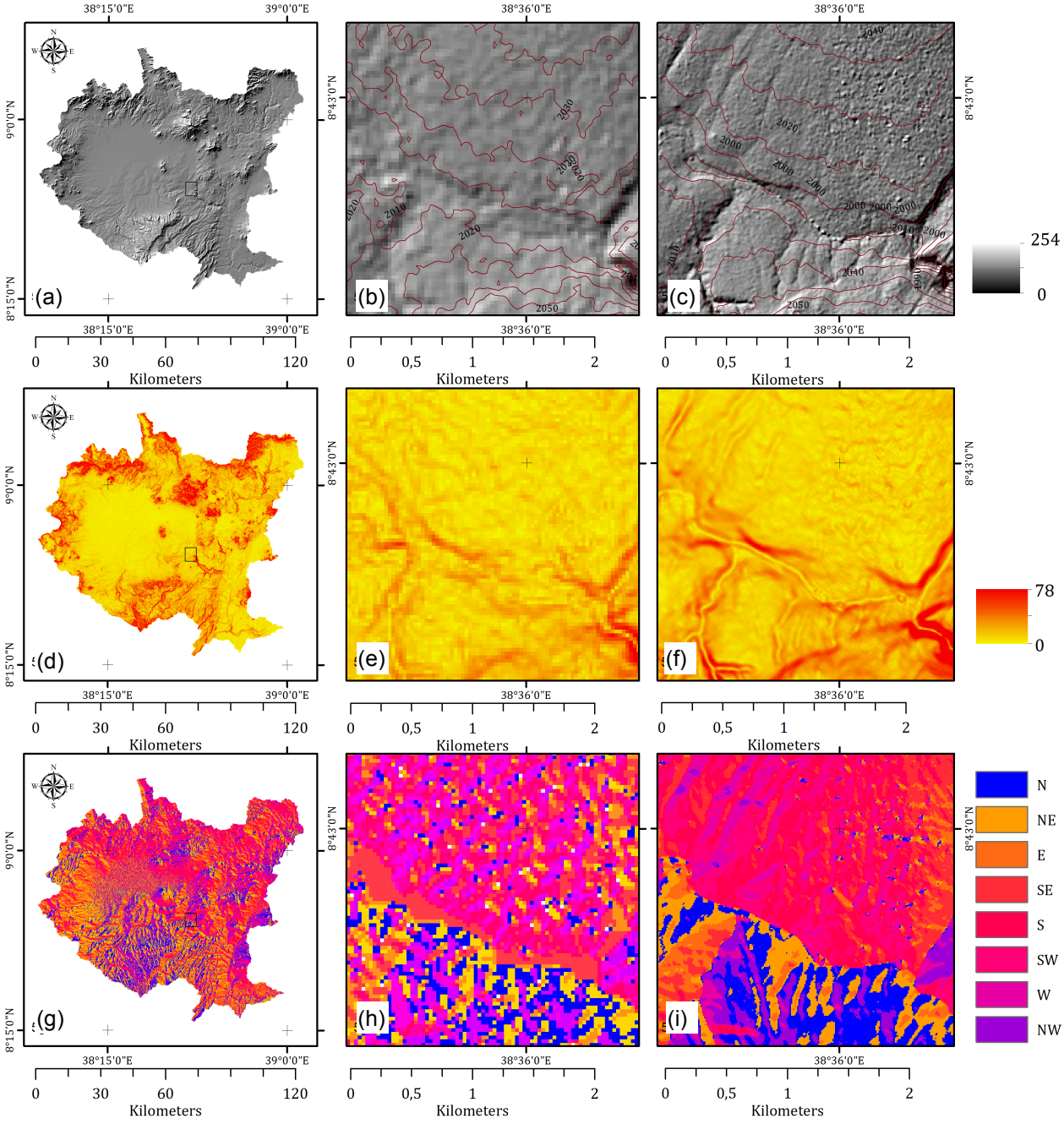

Figure 5. Hillshade maps of the Upper Awash catchment: (a) 90 m spatial resolution SRTM DEM; (b) SRTM-C (2014) 30 m spatial resolution with contour lines; (c) SfM DEM 2 m spatial resolution with contour lines. Slope maps: (d) 90 m spatial resolution SRTM DEM; (e) SRTM-C (2014) 30 m spatial resolution; (f) SfM DEM 2 m spatial resolution. Aspect maps: (g) 90 m spatial resolution SRTM DEM; (h) SRTM-C (2014) 30 m spatial resolution; (i) SfM DEM 2 m spatial resolution.

Slope

Terrain Analysis > Morphometry > Slope, Aspect, Curvature

Figures 5a, 5b and 5c show the gain in resolution of slope gradient with the increase in the DEM spatial resolution, with slope maps of the same resolutions shown in Figures 5d, 5e and 5f. It is an important parameter for models that are used to predict water flows, flooding, erosion, construction, geology, insulation or soil depth.

Aspect

Terrain Analysis > Morphometry > Slope, Aspect, Curvature

The aspect map was reclassified following the division of 360 degrees into quadrants and sub dials:

N	:	0 - 22.5°
NE	:	22.5 - 67.5°
E	:	67.5 - 112.5°
SE	:	112.5 - 157.5°
S	:	157.5 - 202.5°
SW	:	202.5 - 247.5°
W	:	247.5 - 292.5°
NW	:	292.5 - 337.5°
N	:	337.5 - 359.5°

The latter produce 8 possible orientation classes (Figure 5g, 5h and 5i).

Plan and profile curvature

Terrain Analysis > Morphometry > Slope, Aspect, Curvature

Plan Curvature is the horizontal curvature, intersecting with the XY plane. Negative values coincide with concave features. These morphologies are normally produced and/or used for the water to flows. Figures 6a, 6b and 6c clearly shows the river network where blue (or negative curvature values) have been calculated.

Profile curvature is the curvature intersecting with the plane defined by the Z-axis and maximum gradient direction. Positive values describe convex profile curvature, with negative values representing a concave profile, and units are expressed in [1/m]. Figure 6d, 6e and 6f shows the river flowing where curvatures assume negative values, or alternatively where curvature is concave.

SD of elevation (Roughness)

Modules->Grid >Filter > Multi Direction Lee Filter > Standard deviation

Figure 6 (6g, 6h and 6i) demonstrates the roughness calculated from the elevation; it assumes high negative values for the incisions and lower values for flat terrains. The SD of elevation detects breaks in terrain steepness and is therefore most suitable at regional scales while the SD of slope enhances noise in the data (such as caused by forest stands)

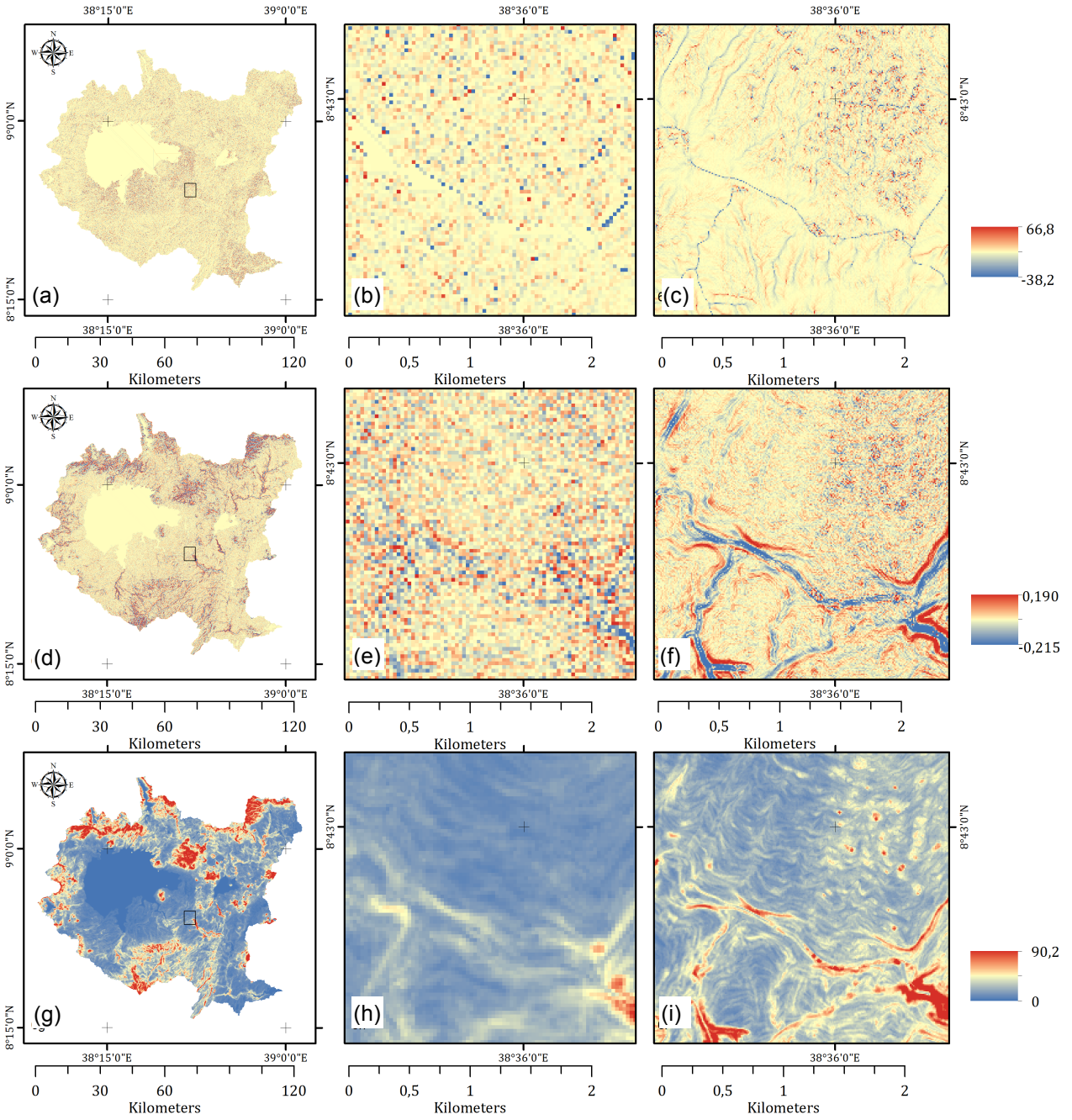

Figure 6. Plan curvature of the Upper Awash catchment at: (a) 90 m spatial resolution based on SRTM DEM; (b) SRTM-C DEM (2014) at 30 m spatial resolution; (c) SfM DEM at 2 m spatial resolution. Profile curvature at: (d) 90 m spatial resolution based on SRTM DEM; (e) SRTM-C DEM (2014) at 30 m spatial resolution; (f) SfM DEM at 2 m spatial resolution. Standard Deviation of elevation (roughness) maps based on: (g) 90 m spatial resolution based on SRTM DEM; (h) SRTM-C DEM (2014) at 30 m spatial resolution; (i) SfM DEM at 2 m spatial resolution.

Catchment area

Terrain Analysis>Hydrology > Catchment Area

Figure 7 (a, b and c) shows the potential flow directions and soil moisture distribution of the study area. The flow tracing algorithm was used, which traces the flow of each cell in a DEM separately until it finally leaves the DEM or ends in a sink. Since the amount of moisture along the hillslope tends to increase from upslope to downslope, additional moisture contributed from upslope as the catchment area increases to the bottom of the valleys. Moisture distribution usually follows a logarithmic scale.

Strahler order

Terrain Analysis > Channel > Strahler order

Figure 7d, 7e and 7f) shows the Strahler order classification. Strahler scheme begins with the smallest channels being classified as 1st order streams. Under such a system the highest order generated form the classification is used to classify the drainage basin or the area of interest, for example the Upper-Awash River can be consider as a seventh order. Good results in terms of perennial streams identification have been achieved for both the 90 m and 30 m DEMs (Figures 7d and 7e), whilst the headwater perennial streams are not well identified within the 2 m SfM DEM (Figure. 7f).

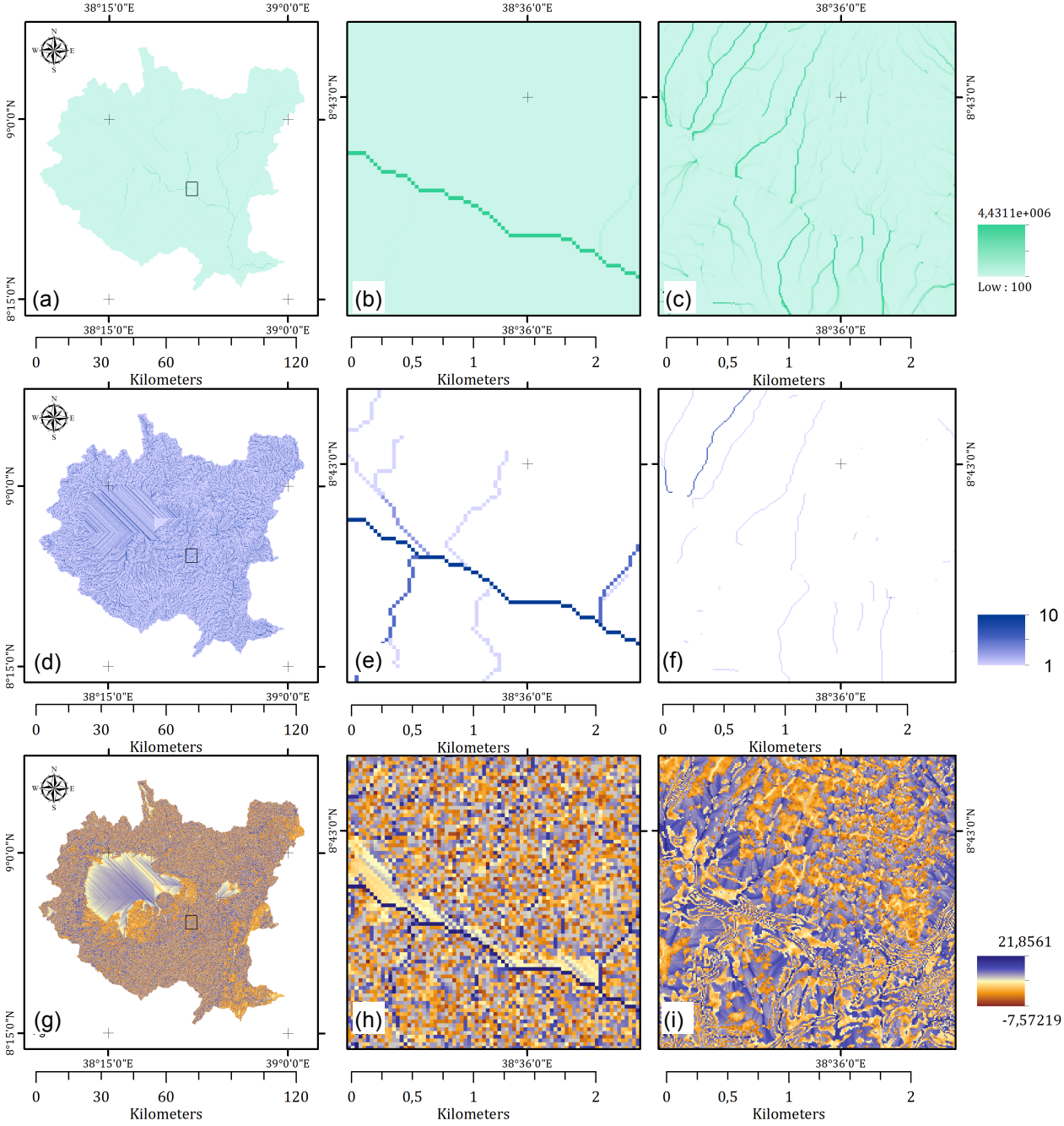

Figure 7. Catchment area of the Upper Awash catchment at: (a) 90 m spatial resolution based on SRTM DEM; (b) SRTM-C DEM (2014) at 30 m spatial resolution; (c) SfM DEM at 2 m spatial resolution. Strahler network at: (d) 90 m spatial resolution based on SRTM DEM; (e) SRTM-C DEM (2014) at 30 m spatial resolution; (f) SfM DEM at 2 m spatial resolution. Topographic wetness index TWI: (g) 90 m spatial resolution based on SRTM DEM; (h) SRTM-C DEM (2014) at 30 m spatial resolution; (i) SfM DEM at 2 m spatial resolution.

Topographic Wetness Index (TWI)

Terrain Analysis > Hydrology > Topographic Wetness Index

Figures 7g, 7h and 7i show the spatial distribution of wetness conditions that result from the contributing areas overland flow, the area drained per unit contour length (and the slope gradient, Eq. 2). It is used to quantify flow intensity and accumulation potential. The TWI index has to be used carefully to predict the distribution of dynamic phenomena, mainly because surface saturation is a threshold process and this diverge from the assumption of a parallel piezometric head gradient (that dictates the direction of subsurface flow) to the land surface. In the reality, surface saturation measurement, would be useful to validate the calculation results.

The study area has been better characterized by the middle resolution SRTM 1arc sec topography, because the mostly flat terrain and the meandering water streams.

Fuzzy Element Landform Classification

Terrain Analysis > Terrain Classification > Fuzzy Element Landform Classification

The fuzzy landform classification is based on the continuous classification method, this groups each pixel according with the grade of membership. It is scale-dependent and identifies different morphometric features (peaks, ridges, passes, channels, pits and planes). The obtained landform classification map successfully shows the distribution of plains, peaks and steep slopes. Attributes used for the classification were elevation, slope, plan curvature, profile curvature, tangential curvature and both maximal and minimal curvature. The continuous classification created 9 classes for the 90 m spatial resolution SRTM C DEM (Figure 8a), 11 classes for the 30 m spatial resolution SRTM C (2014) DEM (Figure 8b) and 2 m SfM DEM (Figure 8c). These are: Back Slope, Spur, Foot Slope, Foot Hollow, Foot Spur, Shoulder Slope, Shoulder Hollow, Shoulder Spur, Plain, Pit and Peak. The maximum membership function provided the degree of landforms characterization into a particular class. (see Figure 8).

Summary

Examples of a general TA workflow (Figure 3) shows a possible approach to calculate the primary and secondary terrain attributes. Selected attributes are presented below at the three chosen spatial resolutions to demonstrate the benefits in landform representation detail:

i. SRTM 90 m shows its strength in the watershed delineation performance and in terms of regional landforms characterization;

ii. SRTM 30 m improved significantly the TA resolution detail because of the better vertical resolution and led to an accurate determination of drainage slopes and precise locations of channels and ridges; and,

iii. TA derived from the 2 m (SfM) DEM shows the fine terrain relief, and the smallest landforms can be derived and offer the best solution for soil erosion modelling issues. It is also possible to delineate sub catchments and define minor drainage networks.

Conclusion

In this chapter, an overview of the particular fields of geomorphology in which TA is of crucial contribution was provided. This is only possible due to the increased availability of near-global DEMs on medium resolution (SRTM 1 arcsec, the forthcoming ALOS PRISM 5 m). The technological progress in terms of sensors and processing techniques (e.g. SfM) allow the transfer of already existing concepts to detailed scales, as well as the potential to develop new ones.

The availability of processing tools improved considerably within the last forty years. Tools

based on sophisticated algorithms are now in the freeware domain. They represent a user-friendly platform that can be used by geomorphologists with a limited knowledge in informatics. Fuzzy landform classification offers non-experts a method to provide information about landforms in terms of their quantitative distribution and degree of uncertainty. It demonstrates how meaningful, spatially coherent landform classes can be achieved from high resolution DEMs.

Temporal variations are encountered in all of the indexes calculations, especially for the highly dynamic areas, (e.g. Rift Valley, fluvial environments, glaciers, deserts). The TA workflow proposed, provides the framework for the assessment of the geomorphological dynamics and can be applied to many heterogeneous environments and multiscale datasets.

It is of crucial importance for geomorphologists to pay close attention to the parameter that influences the hillslope stability, and more broadly to landscape evolution. Both the digital terrain analysis approach and the landform recognition required careful consideration, and even though they are computer based (digital), a significant part of the work has to be carried out in the field to validate the results.

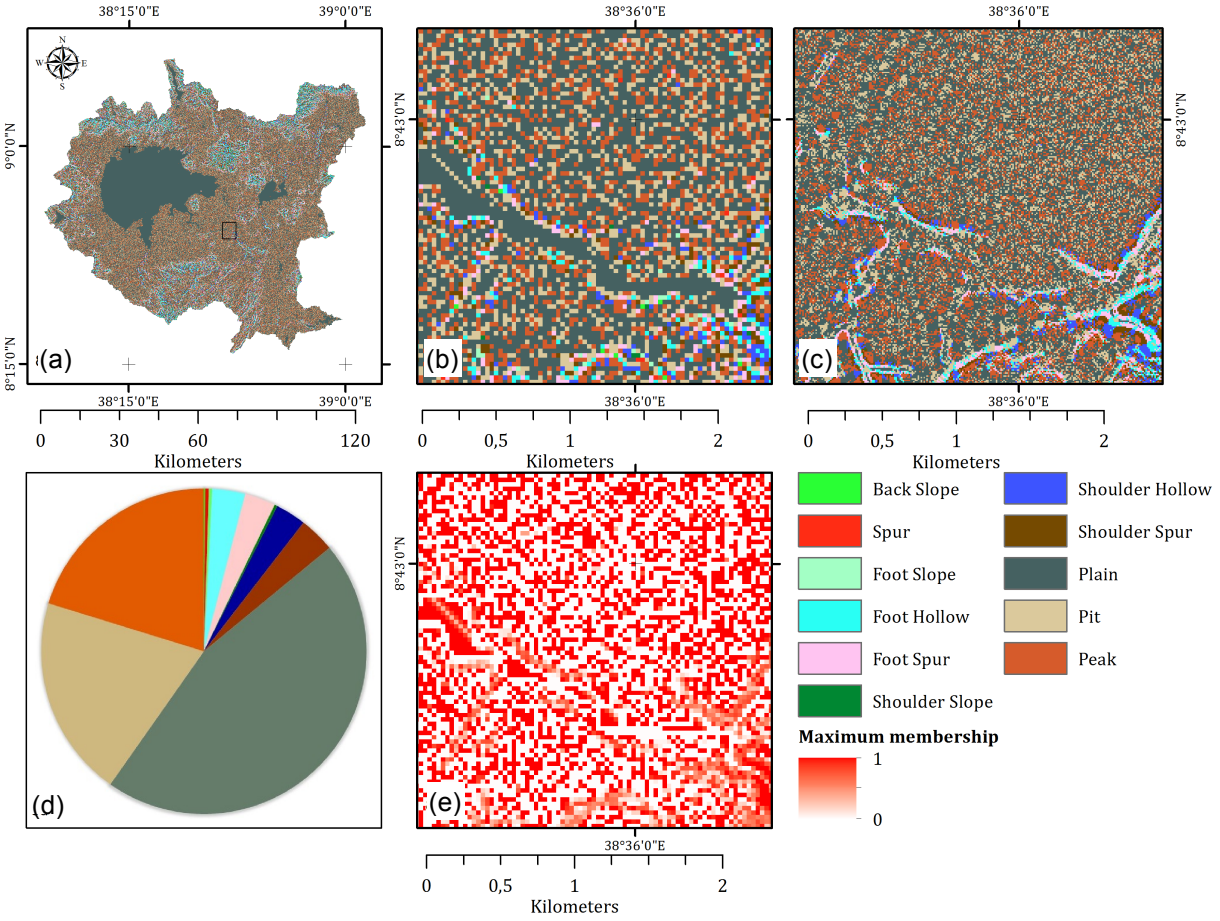

Figure 8. The Fuzzy landform classification of the Upper Awash catchment at: (a) 90 m spatial resolution (SRTM C); (b) SRTM-C DEM (2014) at 30 m spatial resolution; (c) SfM DEM 2 m spatial resolution; (d) pie chart showing the landform classification results expressed in percentage; and, (e) map of maximum membership - this map expresses the uncertainty of the classification, with this approach no pixels are left unclassified.

Acknowledgments

The authors thank the anonymous reviewers that helped us to refine this chapter. We also express our gratitude to the Editors of this Book Dr Lucy Clarke. Data collection was carried out by Dr Jan Kropáček and Calogero Schillaci, in the frame of the project

"Integrated assessment of geomorphological processes dynamics on different spatio-temporal scales in the Ethiopian Highlands using remote sensing and advanced modelling approaches" financed by the DFG-Deutsche Forschungsgemeinschaft (Grant number: HO-1840/11-1). Sincere thanks are also given to Prof. Volker Hochschild, Dr. Michael Märker and our Computer administrator Christian Bick, at the Geosciences Department, University of Tuebingen.

References

Abera W, Antonello A, Franceschi S, Formetta G, Rigon R. 2014. Section 2.4.1: The uDig Spatial Toolbox for hydro-geomorphic analysis. In: Clarke L, Nield J. (Eds.) *Geomorphological Techniques (Online Edition)*. British Society for Geomorphology: London, UK.

Band LE. 1993. Extraction of channel networks and topographic parameters from digital elevation data In: Beven K, Kirkby MJ (Eds.) *Channel Network Hydrology*. Wiley: New York, USA, 13-42.

Band LE. 1986. Topographic partition of watersheds with digital elevation models. *Water Resources Research* **22**: 15-24.

Beven KJ, Kirkby MJ, Seibert J. 1979. A physically based, variable contributing area model of basin hydrology. *Hydrolological Science Bulletin* **24**: 43-69.

Brabyn L. 1998. GIS analysis of macro landform. *The 10th Colloquium of the Spatial Information Research Centre: University of Otago, New Zealand*, 35-48.

Chairat S, Delleur JW. 1993. Integrating a physically based hydrological model with GRASS. In: Kovar K, Nachtnebel HP. (Eds.) *HydroGIS 93: Application of Geographical Information Systems in Hydrology and Water Resources*. International Association of Hydrological Sciences, IAHS Publ. No. 211: Vienna, 143-150.

Cimmery V. 2010a. *SAGA User Guide, updated for SAGA version 2.0.5*. Volume 1: An introduction to the graphical user interface of SAGA. Online common licenced.

Cimmery V. 2010b. *SAGA User Guide, updated for SAGA version 2.0.5.* Volume 2: 'How To' information on many SAGA modules, functions, and GIS applications. Online common licensed.

Dehn M, Gartner H, Dikau R. 2001. Principles of semantic modeling of landform structures. *Computers and Geosciences* **27(8)**: 1005-1010.

Dikau R. 1989. The application of a digital relief model to landform analysis in geomorphology. In: Raper J. (Ed.) *Three Dimensional Application in Geographic Information Systems*. Taylor & Francis: London, UK, 51-77.

Evans IS. 2012. Geomorphometry and landform mapping: What is a landform? *Geomorphology* **137(1)**: 94-106. DOI:10.1016/j.geomorph.2010.09.029.

Farr TG, Rosen PA, Caro, E, Crippen R, Duren R,, Hensley S, Kobrick, M, Paller, M, Rodriguez, E, Roth, L, Seal D, Shaffer S, Shimada J, Umland J, Werner M, Oskin M, Burbank D, Alsdorf D. 2007. The Shuttle Radar Topography Mission. *Review of Geophysics* **45**: RG2004. DOI:10.1029/2005RG000183.

Florinsky I. 2012. *Digital Terrain Analysis in Soil Science and Geology*. Elsevier Academic Press: Oxford, UK.

Fogg GA. 1985. Contour to rectangular grid conversion using minimum curvature. *Computer Vision, Graphics, and Image Processing* **28**: 85-91.

Garbrecht, J, Martz LW. 2000. Digital elevation model issues in water resources modeling. In: Maidment D, Djokic D. (Eds.) *Hydrologic and Hydraulic Modeling Support with Geographic Information Systems.* ESRI Press: Redlands, USA, 1-28.

Gilvear DJ, Bryant RG, Hardy TB. 1999. Application of remote sensing to the study of channel morphology. *Progress in Environmental Science* **1(3)**: 257-284.

Goudie AS. 2004. *Encyclopaedia of Geomorphology*. Routledge: London, UK.

Graf WL. 1987. *Geomorphic systems of North America*. Geological Society of America: Boulder, USA.

Grohmann CH, Smith MJ, Riccomini C. 2010. Multiscale Analysis of Topographic Surface Roughness in the Midland Valley, Scotland. *Geoscience and Remote Sensing* **49(4)**: 1-14.

Haider, VL., Kropáček, J, Dunkl, I, Wagner, B, von Eynatten, H. 2015. Identification of peneplains by multi-parameter assessment of digital elevation models. *Earth Surface Processes and Landforms*, (in print). doi: 10.1002/esp.3729

Hengl TG, Gruber S, Shrestha DP. 2003. *Digital Terrain Analysis in ILWIS*. Lecture Notes and User Guide: https://www.itc.nl/library/Papers_2003/misca/hengl_digital.pdf

Hobson RD. 1972. Surface roughness in topography: quantitative approach. In: Chorley RJ (Ed.) *Spatial Analysis in Geomorphology*. Methuer: London, UK, 225-245.

Horton RE. 1945. Erosional development of streams and their drainage basins, hydrophysical approach to quantitative morphology. *Geological Society of America Bulletin* **56**: 275-370.

Hutchinson, MF, Gallant, JC, 1999. Representation of terrain. In: Longley PA, Goodchild MF, Maguire DJ, Rhind DW. (Eds.) *Geographical Information Systems: Principles, Technical Issues, Management Issues and Applications (2nd Edition)*. Wiley: New York, USA, 105-124.

Irvin BJ, Ventura SJ, Slater BK. 1997. Fuzzy and isodata classification of landform elements from digital terrain data in Pleasant Valley, Wisconsin. *Geoderma* **77**: 137-154.

Javernick L, Brasington J, Caruso B. 2014. Modelling the topography of shallow braided rivers using Structure-from-Motion photogrammetry. *Geomorphology* **213**: 166-182. DOI: 10.1016/j.geomorph.2014.01.006.

Jenson SK, Domingue JO. 1988. Extracting Topographic Structure from Digital Elevation Data for Geographic Information System Analysis. *Photogrammetric Engineering and Remote Sensing* **54(11)**: 1593-1600.

Klimaszewski M. 1982. Detailed geomorphological maps. *ITC Journal* **1982-3**: 265-271.

Large A, Heritage G. 2012. Ground based LiDAR and its application to the characterisation of fluvial forms. In: Carbonneau PE, Piégay H. (Eds.) *Fluvial Remote Sensing for Science and Management*. John Wiley & Sons Ltd: Chichester, UK. DOI: 10.1002/9781119940791.ch14

Lehmann JG. 1816. Die Lehre der Situation-Zeichnung, oder Anweisung zum richtigen Erkennen und genauen Abbilden der Erdoberfläche in topographischen Karten und Situation-Planen.

Lukas K, Weibel R. 1995. Assessment and improvement of methods for analytical hillshading. *Proceedings of the 17th International Cartographic Conference* Barcelona, Spain: 2231-2240: http://icaci.org/files/documents/ICC_proceedings/ICC1995/PDF/Cap430.pdf

McIlroy de la Rosa J. 2012. Section 6.1: Karst Landform Classification Techniques In: Clarke LE, Nield J.M. (Eds.) *Geomorphological Techniques (Online Edition)*. British Society for Geomorphology: London, UK.

McBratney AB, De Gruijter JJ. 1992. A continuum approach to soil classification by modified fuzzy k–means with extragrades. *Journal of Soil Science* **43**: 159-175.

Marida KV. 1972. Statistics of directional data. *Journal of the Royal Statistical Society. Series B (Methodological)* **37(3)**: 349-393.

Märker M, Pelacani S, Schröder B. 2011. A functional entity approach to predict soil erosion processes in a small Plio-Pleistocene Mediterranean catchment in Northern Chianti, Italy. *Geomorphology* **125**: 530-540.

Marston BE, Jenny B. 2015 Improving the representation of major landforms in analytical relief shading. *International Journal of Geographical Information Science*: DOI:10.1080/13658816.2015.1009911.

Marzolff I, Poesen J. 2009. The potential of 3D gully monitoring with GIS using high-resolution aerial photography and a digital photogrammetry system. *Geomorphology* **111**: 48-60.

Milne JD, Clayden B, Singleton PL, Wilson AD. 1995. *Soil Description Handbook*. Manaaki Whenua Press, Landcare Research: Lincoln, New Zealand.

Minár J, Evans IS, Krcho J. 2013. Geomorphometry: Quantitative Land-Surface Analysis. In: Schroder JF (Ed.) *Treatise on Geomorphology*. Academic Press: San Diego, USA, 22-34. DOI:10.1016/B978-0-12-374739-6.00370-5.

O'Callaghan JF, Mark DM. 1984. The extraction of drainage networks from digital

elevation data. *Computer Vision, Graphics, and Image Processing* **28**: 323-344.

Pavlopoulos K, Evelpidou N, Vassilopoulos A. 2009. *Mapping Geomorphological Environments*. Springer: Berlin, Germany.

Peucker TK, Douglas DH. 1975. Detection of surface-specific points by local parallel processing of discrete terrain elevation data. *Computer Graphics and Image Processing* **4**: 375-387.

Pike, RJ, Evans IS, Hengl T. 2008. Geomorphometry: a Brief Guide. In: Hengl, T. and Reuter, H.I. (Eds), Geomorphometry: Geomorphometry: Concepts, Software, Applications. Developments in Soil Science, vol. 33, Elsevier, 1-28 pp.

Prima OD, Echigo A, Yokoyama R, Yoshida T. 2006. Supervised landform classification of Northeast Honshu from DEM-derived thematic maps. *Geomorphology* **78**: 373-386.

Ramasamy SM, Paul MA. 2005. Aid of remote sensing in fluvial geomorphic mapping. In: Ramasamy SM. (Eds.) *Remote Sensing in Geomorphology*. New India Publishing Agenda: New Dehli, India, 98-106.

Schumm SA. 1979. 'Ergodic' reasoning in geomorphology:time for a review of the term? *Transactions of the Institute of British Geographers* **4(4)**: 485-515.

Shary PA. 1991. The second derivative topographic method. In: Stepanov I. (Ed.) *The Geometry of the Earth Surface Structures*. Pushchino Research Centre Press: Pushchino, USSR.

Sidorchuk A, Märker M, Moretti S, Rodolfi G. 2003. Gully erosion modelling and landscape response in the Mbuluzi River catchment of Swaziland. *Catena* **50**: 507-525.

Skidmore AK. 1989. A comparison of techniques for calculating gradient and aspect from a gridded digital elevation model. *International Journal of Geographical Information Systems* **3(4)**: 323-334.

Smith MJ, Rose J, Gousie MB. 2009. The Cookie Cutter: A method for obtaining a quantitative 3D description of glacial bedforms. *Geomorphology* **108(3-4)**: 209-218. DOI:10.1016/j.geomorph.2009.01.006.

Smith TR, Zhan C, Gao P. 1990. A knowledge-based, two-step procedure for extracting channel networks from noisy DEM data. *Computer Geoscience* **16**: 777-786.

Sørensen RZ, Zinko U, Seibert J. 2006. On the calculation of the topographic wetness index: evaluation of different methods based on field observations. *Hydrology and Earth System Sciences* **10**: 101-112.

Speight JG. 1990. *Australian Soil and Land Survey: Field Handbook* (2nd Edition). Inkata Press: Melbourne, Australia.

Speight JG. 1974. A parametric approach to landform regions. In: Brown EH, Waters RS. (Eds.) *Progress in Geomorphology: Papers in honour of D.L. Linton*. Institute of British Geographers: London, UK, 213-230.

Strahler AN. 1957. Quantitative analysis of watershed geomorphology. *Transactions of the American Geophysical Union* **33**: 913-920.

Tadono T, Ishida H, Oda F, Naito S, Minakawa K, Iwamoto H. 2014. Precise global DEM generation by ALOS PRISM. *ISPRS Annals of the Photogrammetry and Remote Sensing Spatial Information Science* **II-4**: 71-76.

Thornbury WD. 1965. *Regional Geomorphology of the United States*. Wiley: New York, USA.

Valentin C, Poesen J, Yong Li. 2005. Gully erosion: Impacts, factors and control. *Catena* **63 (2-3)**: 132-153.

Wang L, Liu H. 2006. An efficient method for identifying and filling surface depressions in digital elevation models for hydrologic analysis and modelling. *International Journal of Geographical Information Science* **20**: 193-213.

Westoby MJ, Brasington J, Glasser NF, Hambrey MJ, Reynolds JM. 2012. Structure-from-Motion" photogrammetry: A low-cost, effective tool for geoscience applications. *Geomorphology* **179**: 300-314.

Wieczorek GF, Snyder JB. 2009. Monitoring slope movements. In: Young R, Norby L (Eds.) *Geological Monitoring*. Geological Society of America: Boulder, USA, 245-271.

Wilson JP. 2012. Digital terrain modeling. *Geomorphology* **137**: 107-121.

Wilson JP, Gallant JC. 2000. *Terrain Analysis: Principles and Applications*. John Wiley and Sons: New York, USA.

Zadeh LA.1965. Fuzzy Sets. *Information and Control* **8**: 338-358.

Zakerinejad R, Märker M. 2014. Prediction of gully erosion susceptibilities using detailed terrain analysis and maximum entropy modeling: a case study in the Mazayejan Plain, Southwest Iran. *Geografia Fisica e Dinamica Quaternaria* **37**: 67-76.

Zeverbergen LW, Thorne CR. 1987. Quantitative analysis of land surface topography. *Earth Surface Processes and Landforms* **12**: 47-56.

Zhang W, Montgomery DR. 1994. Digital elevation model grid size, landscape representation, and hydrologic simulations, *Water Resources Research* **30**: 1019-1028.

Sitography

Following a list of useful URLs:

CGIAR (Consortium for Spatial Information): http://srtm.csi.cgiar.org/

EROS (NASA): http://eros.usgs.gov/

ESA/AIRBUS: http://www.geo-airbusds.com/

NASA: http://www2.jpl.nasa.gov/srtm/

USGS (Earth Explorer): http://earthexplorer.usgs.gov/